Composites Part B 164 (2019) 368–376

Contents lists available at ScienceDirect

Composites Part B

journal homepage: www.elsevier.com/locate/compositesb

Controllable mechanical properties of epoxy composites by incorporating self-assembled carbon nanotube–montmorillonite

Shaohua Zeng, Mingxia Shen*, Yijiao Xue, Yifei Zheng, Ke Zhang, Yanxin Han, Lu Yang

College of Mechanics and Materials, Hohai University, Nanjing 211100, China

ARTICLE INFO

Keywords:
Hybrid
Polymer-matrix composites (PMCs)
Mechanical properties

ABSTRACT

A self-assembled multi-walled carbon nanotube – montmorillonite (MWCNT – Mt) hybrid wherein varied MWCNTs contents were attached on the exfoliated Mt was constructed and further used to reinforce epoxy composites. By just tuning mass ratios of MWCNT:Mt, the dispersion level of MWCNTs, exfoliation degree of Mt and ultimately mechanical properties of resultant composites could be controlled. The effect of MWCNT – Mt hybrids on structure-property relationships of epoxy composites was investigated. Under an optimal mass ratio of MWCNT:Mt (0.1:1), the toughness of epoxy composites was significantly enhanced, revealing the synergistic toughening effect of MWCNTs and Mt; the tensile and flexural strength of epoxy composites were improved by 26.8% and 20.4%, respectively; the storage modulus in the glassy region increased by 15.8%, compared with epoxy composite containing pristine Mt.

1. Introduction

Epoxy resins (EP) have been widely used in engineering applications due to their good chemical and moisture resistance, low thermal shrinkage and excellent adhesion to many substrates [1,2]. However, with the rapid development of industries such as electronic device, power equipment and aerospace system, the mechanical properties of the cured EP are called for higher requirements. The two-dimensional (2D) sheet-like nanoclays, especially montmorillonite (Mt), have been frequently applied to reinforce epoxies owing to its large surface area, strong adsorption and ion exchange ability and moderate cost [3,4]. The one-dimensional (1D) tube-like multi-walled carbon nanotubes (MWCNTs) are another attractive nanofiller for enhancing properties of epoxies because of their high aspect ratios, large flexibility and high strength and modulus [5–8]. A small amount of Mt or MWCNTs incorporated into EP can give the composites with good mechanical and thermal properties [9–11]. For both 1D and 2D nanofillers, the uniform dispersion and strong interfacial adhesion with epoxy matrices are the challenging issues still [12,13]. Many efforts have been devoted to the intercalation or exfoliation of Mt in EP and several studies have been performed on the functionalization of MWCNTs and their dispersion in EP [14,15].

Considering their special structures and properties, the incorporation of both Mt and MWCNTs into polymeric matrices has been studied in the past decade [16,17]. The polymer-matrix hybrid composite containing Mt and MWCNTs show superior properties when compared with that filled with individual Mt and MWCNTs due to their synergistic effect. The most widely used method for the preparation of hybrid composites is to simply disperse Mt and MWCNTs separately in the liquid resin [18,19]. Unfortunately, this method is only suitable for low loadings of Mt and MWCNTs because the viscosity of Mt/MWCNTs/resin suspensions increases at high loadings [20]. Moreover, at high loadings of Mt and MWCNTs, the exfoliation of Mt and dispersion of MWCNTs in resins remain difficult even through these nanofillers have been functionalized.

For overcoming the aforementioned shortcomings, a combination of MWCNTs and Mt to form 1D/2D hybrid nanomaterials has attracted considerable attention [21]. These MWCNTs/Mt hybrids can not only improve the dispersibility of Mt and MWCNTs in polymeric matrix but also enhance the interfacial interactions with the matrix. Several techniques have been used to prepare the MWCNTs/Mt hybrids, such as chemical vapor deposition (CVD) [22,23], dry grinding [24,25], and layer-by-layer assembly [26,27]. Although extensive work has proven that MWCNTs/Mt hybrids can play a positive role in their dispersion and the properties of corresponding polymers, only a few has focused on the effect of MWCNTs/Mt hybrids on mechanical properties of epoxy composites.

Previously, the hybridization of Mt and MWCNTs was performed by a simple yet effective self-assembly method [28]. Although the MWCNT – Mt hybrids were dispersed well in epoxy, the mechanisms of

* Corresponding author. College of Mechanics and Materials, Hohai University, Nanjing, 211100, China.
E-mail address: mxshen@hhu.edu.cn (M. Shen).

https://doi.org/10.1016/j.compositesb.2018.12.028
Received 27 September 2018; Received in revised form 20 November 2018; Accepted 11 December 2018
Available online 12 December 2018
1359-8368/

MWCNTs on the exfoliation of layered Mt were not investigated deeply. Inspired by this, the nanostructured hybrid wherein varied MWCNTs contents were adsorbed on the surface of Mt was prepared here. A systematic investigation was performed to study the effect of MWCNT:Mt mass ratios on the structure and dispersibility of MWCNT − Mt hybrids and mechanical properties of corresponding epoxy composites. Furthermore, synergistic toughening mechanisms of MWCNT − Mt hybrids for epoxy composites were also discussed. This study demonstrates that the controllable mechanical properties can be achieved through the structure-based design of MWCNT–Mt hybrids.

2. Experimental

2.1. Materials

Mt (FH − F3w; purity: ≥95%; cation exchange capacity: ~110 mmol/100 g) was produced by Zhenjiang Fenghong New Material Co., Ltd (Huzhou, China). Carboxyl MWCNTs (carbon: ≥90%, diameter: 20–40 nm, length: ~30 μm, −COOH content: ~1.43 wt.%) were purchased from Chengdu Organic Chemicals Co., Ltd. (Chengdu, China). The bisphenol-A type epoxy resin (Araldite LY 1564 SP; viscosity: 1200–1400 mPa s) and its amine hardener (Aradur 3486; viscosity: 10–20 mPa s) were provided by Huntsman Advanced Materials Americas Inc. (Texas, USA). The chemicals including *N,N*-dimethylformamide (DMF), 1-hydroxybenzotriazole (HOBt), triethylenetetramine (TETA), diisopropylcarbodiimide (DIC) and concentrated hydrochloric acid (HCl) were supplied by Nanjing Chemical Reagent Co., Ltd (Nanjing, China).

2.2. Preparation of self-assembled MWCNT–Mt

The MWCNT–Mt hybrid was prepared by a self-assembly method [28], following the procedures:

(1) 10 mg HOBt, 10 mg DIC and 500 mg carboxyl MWCNTs were dispersed into 100 mL DMF using an ultrasonic bath (600 W) for 0.5 h. 250 mg TETA was then dissolved into the above suspension, followed by slowly stirring at room temperature for 24 h. Subsequently, the amino-functionalized MWCNTs were obtained after filtrating and then washing with deionized water three times.
(2) Amino-functionalized MWCNTs were ultrasonically dispersed in 100 mL deionized water, and 10 mL HCl was then added dropwise with stirring. After stirring for 0.5 h, the TETA salts-grafted MWCNTs were obtained.
(3) 1000 mg Mt was dispersed in 40 mL deionized water using an ultrasonic bath (600 W) for 0.5 h and then stirred at 80 °C for 0.5 h.
(4) The treated Mt and TETA salts-grafted MWCNTs were mixed with various mass ratios of MWCNT:Mt (0.05:1, 0.1:1 and 0.2:1) and then stirred overnight at 80 °C, respectively. Finally, these filtrates were washed with deionized water three times and dried to get three types of self-assembled MWCNT–Mt, which was marked as MWCNT–Mt(0.05:1), MWCNT–Mt(0.1:1) and MWCNT–Mt(0.2:1), respectively.

To make a comparison, pristine Mt was treated with the same ultrasonic and thermal conditions as self-assembled MWCNT–Mt.

2.3. Fabrication of epoxy composites

A solution intercalation method was used to produce epoxy composites containing Mt − MWCNT hybrids [28]. The epoxy mixture was comprised of 0.5 wt.% of MWCNT − Mt hybrids, 100 wt.% of epoxy resins and 34 wt.% of amine hardeners. First, 0.25 g MWCNT − Mt hybrids were dispersed in 50.0 g epoxy resins by a magnetic stirring for 24 h at 400 rpm and then an ultrasonic water bath (KQ600-KDE; Kunshan Ultrasonic Instruments Co., Ltd, China) for 0.5 h at 600 W. Subsequently, the above mixture was milled on a three-roll mill (EXAKT 50; EXAKT GmbH, Germany) with a maximum rotation speed of 200 rpm. Three passes were performed by varying gaps (20 μm, 10 μm and 5 μm, respectively) between feeding roller and center roller.

Upon completion of three-roll milling, 17.0 g amine hardeners were added in the above mixture while magnetically stirring at 600 rpm for 10 min. After that, the liquid resin suspensions were degassed in a vacuum oven (about −0.1 MPa) at 40 °C for 15 min, and then poured into polytetrafluoroethylene molds, followed by curing at room temperature for 24 h and then post-curing at 80 °C for 8 h.

Following the similar process, the epoxy composite containing 0.5 wt.% Mt (E/Mt) was also prepared. The epoxy composites filled with 0.5 wt.% of MWCNT–Mt(0.05:1), MWCNT–Mt(0.1:1) and MWCNT–Mt(0.2:1) were marked as E/M-Mt(0.05:1), E/M-Mt(0.1:1) and E/M-Mt(0.2:1), respectively.

2.4. Characterization

Fourier transform infrared (FTIR) spectra was recorded using a Vertex 80v FTIR spectrometer (Bruker, Germany) within the wave numbers range of 400–4000 cm^{-1}. Energy dispersive X-ray spectrometer (EDX; EX-250, Horiba, Japan) was used to explore the element distribution in the interface regions between Mt and MWCNTs. Field-emission scanning electron microscopy (SEM; SU8010, Hitachi, Japan) was performed to investigate the surface morphology of nanofillers and fracture surface of epoxy composites. All the observed samples were coated with a layer of gold before tests.

The microstructure of the nanofillers and their dispersion in epoxy composites were detected using transmission electron microscopy (TEM; JEM-1400, JEOL, Japan). X-ray diffraction (XRD; ARL-X'TRA, Thermo Scientific, USA) was used to examine structural changes of the nanofillers and corresponding composites, operating at room temperature with Cu-target Kα radiation (λ = 0.154 nm). The thermal gravimetric (TG) and differential thermal gravimetric (DTG) analysis of the nanofillers were evaluated by thermogravimetric analyzer (Pyris 1 TGA, PerkinElmer Inc., USA) at a heating rate of 10 °C/min from room temperature to 800 °C in an air atmosphere.

The tensile and flexural tests were conducted using a universal testing machine (Model 3343, Instron Corp., Canton, Mass., USA) in referring to ISO 527-2:2012 and ISO 178:2010, respectively. Both tests were carried out at room temperature and the effective data were the average of five specimens for each composite. Dynamic mechanical thermal analysis (DMTA) was conducted using a TA instruments Q800 machine (USA) under air. DMTA tests were performed under three-point bending mode at a frequency of 1 Hz and a heating rate of 5 °C/min from room temperature to 180 °C.

3. Results and discussion

3.1. Structure and morphology of MWCNT–Mt

FTIR spectra of Mt, carboxyl MWCNTs and MWCNT–Mt with various mass ratios are shown in Fig. 1. For the Mt, the peak at 3632 cm^{-1} is attributed to the O–H stretching of lattice water in Mt, and the peaks at 3436 cm^{-1} and 1640 cm^{-1} are assigned to stretching and deformation vibrations of –OH [29]. The peaks at 3436 cm^{-1} and 1705 cm^{-1} are ascribed to the stretching vibrations of –OH and C = O, respectively, both of which come from –COOH moieties on carboxyl MWCNTs [11,30]. Significantly, the peak intensity of three types of MWCNT − Mt at 3436 cm^{-1} is higher than that of carboxyl MWCNTs, presumably due to the overlapping of –OH and –NH– stretching vibrations. The bending vibration of C–N appears at 1157 cm^{-1}. The peaks at 2931, 2853 and 1463 cm^{-1} are indicative of $–CH_2–$ stretching and bending vibrations, arising from the TETA salts. Furthermore, the peak intensities of –NH– and $–CH_2–$ are enhanced with the increase of MWCNT contents in hybrids. The existence of these bonds (i.e., C = O, –NH–, C–N and $–CH_2–$)

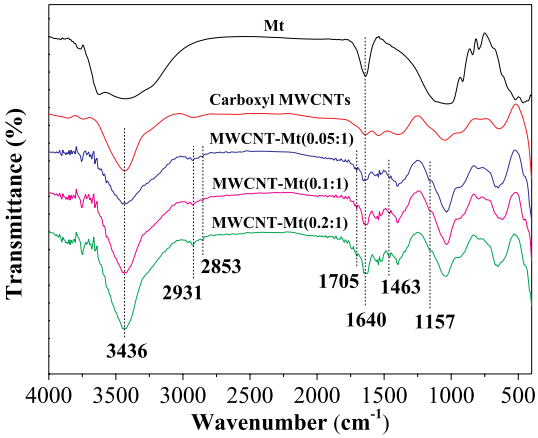

Fig. 1. FTIR spectra of Mt, carboxyl MWCNTs and MWCNT − Mt hybrids with different mass ratios.

indicates that TETA salts are chemically linked on the MWCNTs surface.

For evaluation of the interaction between Mt and MWCNTs, all the types of MWCNT − Mt hybrids were investigated by SEM and EDX, as displayed in Fig. 2. The element C comes from the additives in Mt, carboxyl MWCNTs or TETA, and the elements Mg and Ca arise from Mt. Specially, the element N existed in MWCNT–Mt mainly comes from TETA. With the introduction of TETA salts-grafted MWCNTs, the C% for MWCNT–Mt is raised by 1.58–2.64 times; element N content is improved to 9.37–20.29%; the total amount of Mg and Ca are significantly reduced, as compared with those of Mt. Moreover, as the TETA salts-grafted MWCNTs increase, both C% and N% are raised while the total amount of Mg and Ca exhibit a down-trend. These data indicate that TETA salts-grafted MWCNTs can be assembled on the surface of Mt sheets by a cation-exchange reaction; a strong interfacial bond between Mt and MWCNT is successfully achieved.

The structures of Mt and MWCNT–Mt with different mass ratios were detected by XRD, as shown in Fig. 3(a). A sharp diffraction peak at about 7.07° in pristine Mt is observed, which is attributed to the 001 reflection. For the MWCNT–Mt, the 001 reflection of Mt is shifted to 4.07°–4.75°, suggesting that the d_{001} spacing of Mt is expanded. It indicates that TETA molecules grafted on the MWCNTs are inserted into the layered Mt and thus pre-exfoliate Mt. This result can be further identified from TEM images (see Fig. 3(b)). It is evident that the Mt in MWCNT–Mt(0.1:1) exhibits the transparent sheet and MWCNTs are uniformly dispersed on the Mt sheet. In contrast, some Mt sheets are stacked in MWCNT–Mt(0.05:1) when the MWCNTs content is low; however, at high MWCNTs contents, the MWCNTs are bundled in MWCNT–Mt(0.2:1) although no stacked Mt sheets are found. These results demonstrate that TETA salt-modified MWCNTs can assist in the pre-exfoliation of Mt sheets.

In order to evaluate the thermal stability of MWCNT–Mt hybrids and corresponding amounts of MWCNTs, all the hybrids were investigated by thermogravimetric analysis, as presented in Fig. 4. The Mt shows two major mass losses, which occurred at around 38 °C and 500 °C, respectively. The first mass loss (approximately 15%) reveals the release of crystal water within clay minerals and the second mass loss (approximately 3%) is attributed to the dehydroxylation of the aluminosilicate [31]. The residual mass at over 700 °C corresponds to the clay. As seen in Fig. 4(a), initial decomposition temperature of MWCNT–Mt hybrids is lower than that of pristine Mt. Due to the incorporation of a small number of MWCNTs, the thermal stability of MWCNT–Mt(0.05:1) is significantly reduced. With the increase of MWCNTs, the mass loss rate of MWCNT–Mt hybrids decreases when the temperature is over 100 °C, which is attributed to the synergistic effect of MWCNTs and Mt. It is also noted that a significant mass drop occurs between 500 °C and 700 °C, indicating the decomposition of MWCNTs and dehydroxylation of Mt. During this decomposition process, the samples MWCNT–Mt(0.05:1), MWCNT–Mt(0.1:1) and MWCNT–Mt (0.2:1) display the mass losses of 6.4%, 10.7% and 16.8% (Fig. 4(a)), corresponding to the oxidation temperatures of 621.9 °C, 632.2 °C and 618.2 °C (Fig. 4(b)), respectively. It can be concluded that the MWCNT–Mt(0.1:1) exhibits the lowest mass loss rate and highest decomposition temperatures, implying superior thermal stability of hybrids.

3.2. Intercalation and dispersion of MWCNT–Mt in composites

The effect of MWCNT–Mt hybrids on the structural phase of epoxy composites was further analyzed by XRD, as shown in Fig. 5(a). The characteristic peak of Mt at 6.1° appears in E/Mt, indicating the presence of stacked Mt in matrix. It is noteworthy that this characteristic peak of Mt is absent in E/M-Mt(0.05:1), E/M-Mt(0.1:1) and E/M-Mt (0.2:1), suggesting the formation of exfoliated Mt in matrix. The broad peak at 17.8° is indicative of the amorphous phase of epoxy matrix [32]. The peak position of epoxy matrix at ~17.8° is more or less unchanged in epoxy composites containing MWCNT–Mt hybrids.

The dispersion of MWCNT–Mt hybrids in epoxy composites was verified by TEM, as displayed in Fig. 5(b). A large number of stacked Mt are still observed in E/Mt. It is also noted that the exfoliated Mt and well-dispersed MWCNTs are observed in E/M-Mt(0.1:1). In contrast, under lower or higher MWCNTs contents in MWCNT–Mt hybrids, some stacked Mt or MWCNTs agglomerates are observed, respectively. These results indicate that the introduction of MWCNTs can be helpful for dispersion and exfoliation of Mt in matrix; meanwhile, the Mt sheets also facilitate the dispersion of MWCNTs in matrix. However, the high content of MWCNTs in MWCNT–Mt hybrids is highly susceptible to incur the re-agglomeration of MWCNTs.

3.3. Tensile properties of composites

The typical stress–strain curves of tensile tests and the results of tensile properties including tensile strength, Young's modulus and elongation at break are shown in Fig. 6. It is evident from Fig. 6(a) that the incorporation of MWCNT–Mt in epoxy can significantly enhance the tensile properties. With increasing MWCNTs contents, the tensile properties of MWCNT–Mt-filled epoxy composites increase at first and then begin to decline as the mass ratio of MWCNT:Mt reaches to 0.1:1 (see Fig. 6(b) and (c)). Compared with the E/Mt without MWCNTs, the tensile strength and Young's modulus of E/M-Mt(0.1:1) are enhanced by 26.8% and 18.8%, respectively. These results are attributed to the homogeneous dispersion of MWCNT–Mt in matrix and strong interfacial adhesion between MWCNT–Mt and matrix. Moreover, the highly dispersed MWCNTs not only promote the exfoliation degree of Mt sheets in matrix but also cause uniform stress distribution. However, the decreased tensile properties under high MWCNTs contents are ascribed to the re-agglomeration of MWCNTs in matrix.

Also, the incorporation of MWCNT–Mt hybrids can lead to a significant effect on the toughness of resultant composites. As seen in Fig. 6(c), the elongation at break of epoxy composites exhibits an up-trend with increasing MWCNTs contents in hybrids, and a peak value is observed for E/M-Mt(0.1:1), which is 19.7% higher than E/Mt. With further increasing MWCNTs contents in hybrids (i.e., E/M-Mt(0.2:1)), a down-trend is observed. Meanwhile, this result can be further confirmed from the tensile toughness of epoxy composites (see Fig. 6(d)), which can be calculated by integrating the area under the tensile stress-strain curves [33–35]. From Fig. 6(d), the maximum increment of tensile toughness (92.0%) is obtained for E/M-Mt(0.1:1), compared with E/Mt. These results demonstrate that both the interlayer structure of Mt and the flexibility of MWCNTs are beneficial for toughening epoxy composites.

The toughening mechanisms can be further demonstrated from SEM observations, as shown in Fig. 7. The fracture surface of pure EP is

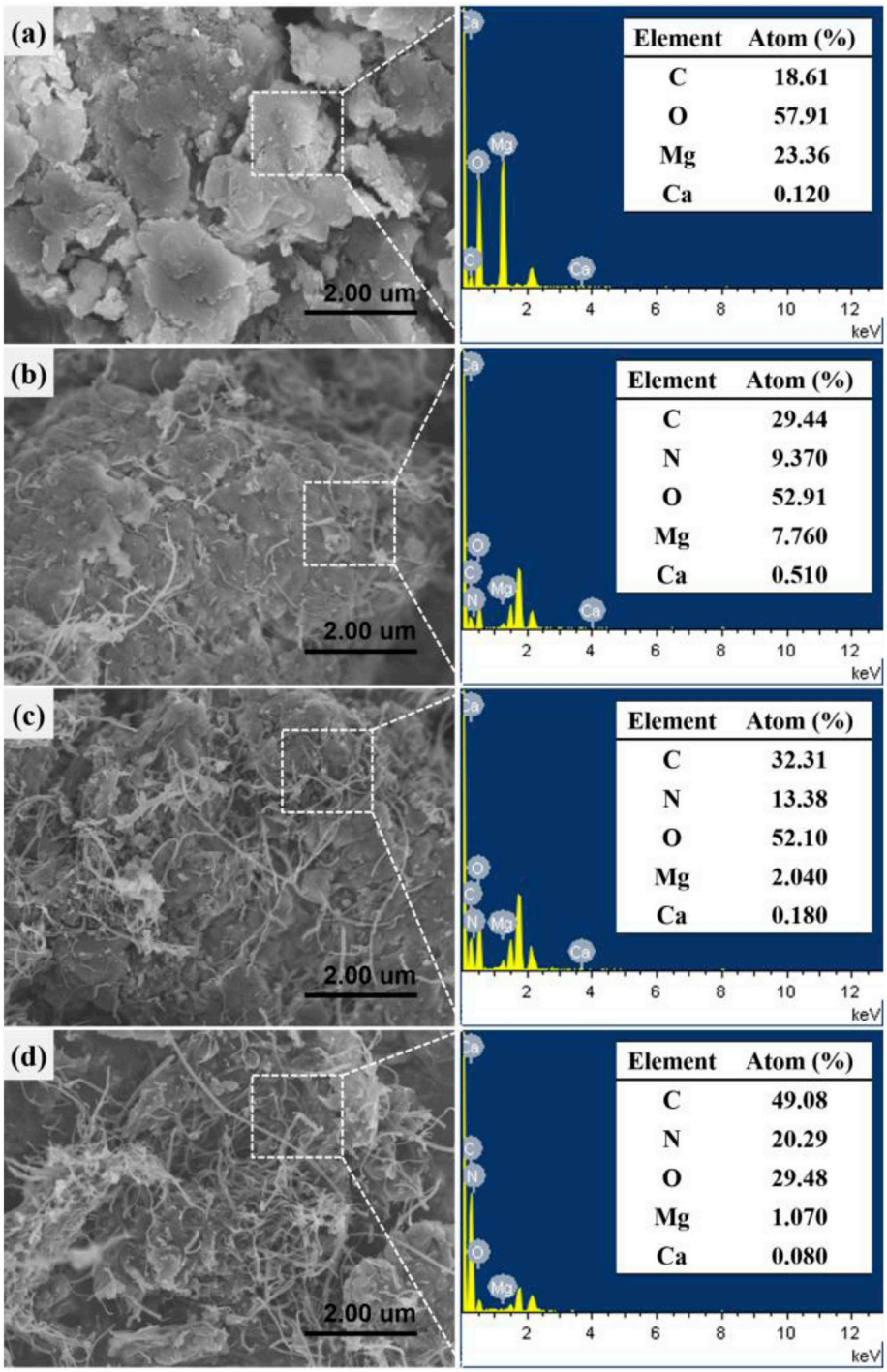

Fig. 2. SEM images and EDX spectrums of (a) Mt, (b) MWCNT–Mt(0.05:1), (c) MWCNT–Mt(0.1:1) and (d) MWCNT–Mt(0.2:1).

relatively flat and smooth (Fig. 7(a)), revealing its brittle nature. By comparison, the fracture surface of epoxy composites becomes rougher and appears some scale-like structures, evidencing the ductile fracture of matrix. Moreover, the average size of the scales reduces with the increase of MWCNTs contents. This is because that the presence of MWCNTs can change the direction of crack propagation [36]. Meanwhile, well-dispersed MWCNTs on the Mt surface can facilitate the stress transfer and dissipate more fracture energy. Therefore, the incorporation of MWCNT–Mt hybrids can yield a synergistic effect on toughening epoxy composites.

The interfacial adhesion between MWCNT–Mt and matrix is also critical to the mechanical properties of epoxy composites. As seen in Fig. 8(a), some obvious gaps (see black arrows) between matrix and stacked Mt are observed in E/Mt, indicating severe interfacial debonding. From Fig. 8(b) and (c), the pulled-out MWCNTs and bridged MWCNTs are observed and no gaps between MWCNT–Mt and matrix are found on the fracture surface. It can be explained that the MWCNTs anchored on the surface of Mt sheets can impart a mechanical interlocking with matrix. Meanwhile, the introduction of functional groups (i.e., amino groups and carboxyl groups) on the MWCNTs surface can increase the wettability and chemical interactions between MWCNT–Mt and epoxy matrix [28,37,38]. However, some agglomerated MWCNTs

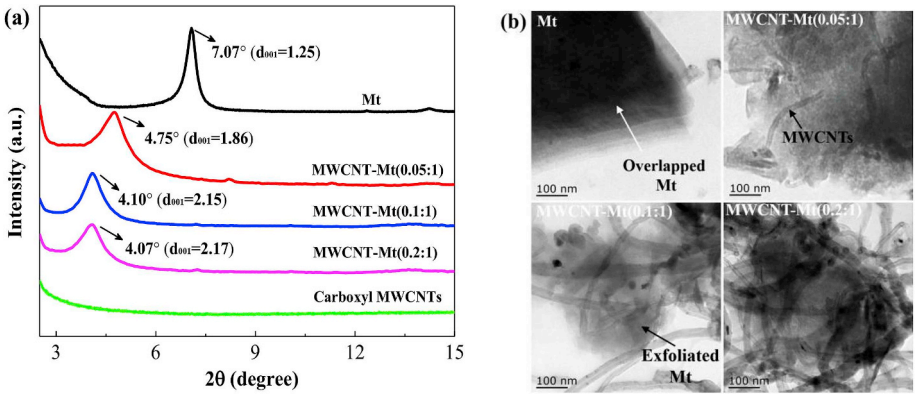

Fig. 3. (a) XRD patterns and (b) TEM images of Mt and MWCNT – Mt hybrids with different mass ratios.

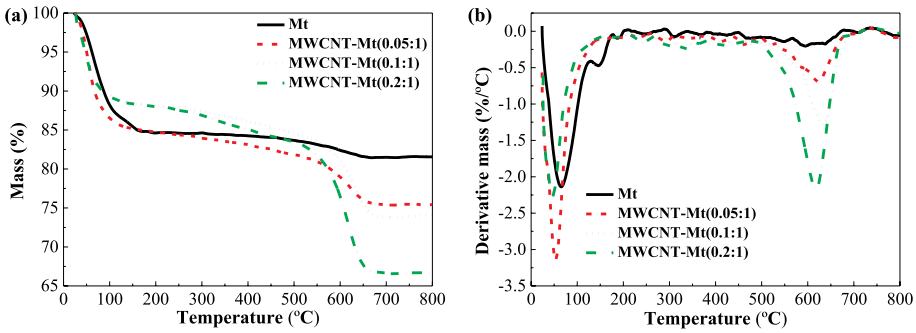

Fig. 4. (a) TG and (b) DTG curves of Mt and MWCNT – Mt hybrids with different mass ratios.

are observed in E/M-Mt(0.2:1) (see Figs. 7(e) and Fig. 8(d)). These MWCNT agglomerates easily induce the stress concentration and thereby produce interface defects, leading to the material failure.

3.4. Flexural properties of composites

To some extent, flexural behavior can reveal the stiffness of materials. The typical stress–strain curves of flexural tests and flexural strength and modulus of epoxy composites containing MWCNT–Mt with various mass ratios are displayed in Fig. 9. The positive effect of MWCNT–Mt incorporation is clearly evident from Fig. 9(a). Similar to tensile properties, a same trend is observed in flexural properties (Fig. 9(b)). Compared with the E/Mt with no MWCNTs, the flexural strength and modulus of E/M-Mt(0.1:1) are raised by 20.4% and 22.3%, respectively. Such significant enhancement in flexural properties is closely associated with the uniform dispersion of MWCNTs on the surface of Mt sheets, high degree of exfoliation of Mt in matrix, and strong interfacial adhesion between MWCNT–Mt and matrix.

3.5. Dynamic mechanical thermal properties of epoxy composites

The micromechanical properties and thermal stability of polymer composites can be revealed from DMTA tests. Fig. 10 shows the curves of storage modulus (E') and loss factor as a function of temperature. The key data are also displayed in Table 1, including E' values at 30 °C in the glassy region (E'_{30}), the temperature at which the E' begins to stabilize in the rubbery region (T_r), peak of loss factor (Tan δ_{max}) and corresponding glass transition temperatures (T_g).

As seen in Fig. 10(a), the role of incorporating MWCNT–Mt in enhancing the E' of epoxy composites in the glassy region is evident.

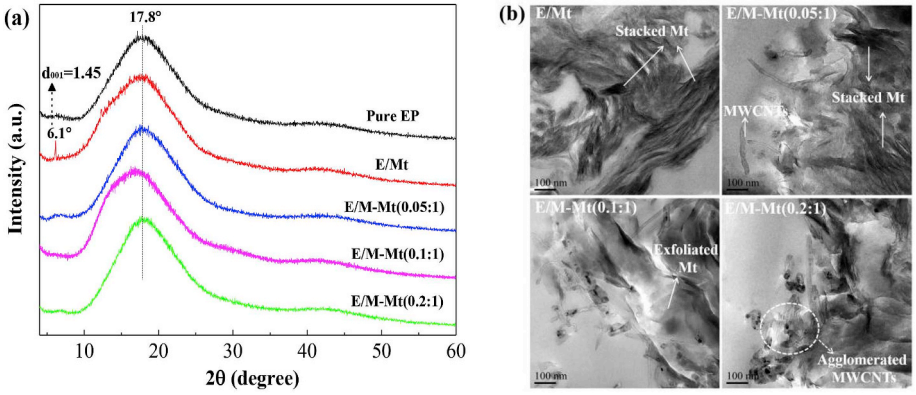

Fig. 5. (a) XRD patterns and (b) TEM images of epoxy composites containing MWCNT – Mt hybrids with different mass ratios.

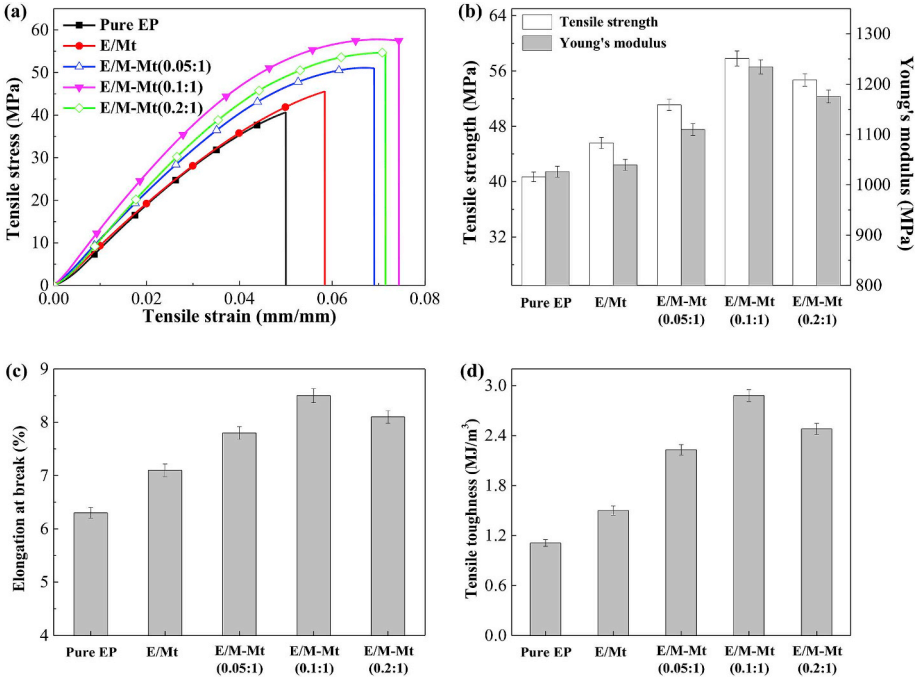

Fig. 6. (a) Stress–strain curves, (b) tensile strength and Young's modulus, (c) elongation at break and (d) tensile toughness of epoxy composites containing MWCNT − Mt hybrids with different mass ratios.

Moreover, with the increase of MWCNTs contents in hybrids, the E'_{30} value of epoxy composites rises to a peak at the MWCNT:Mt mass ratio of 0.1:1 and thereafter declines. The maximum improvement in the E'_{30} value (15.8%) is obtained for E/M-Mt(0.1:1), compared with the E/Mt. It can be well explained by the synergistic reinforcement of Mt and MWCNTs, homogeneous dispersion of MWCNT–Mt in matrix and improved interfacial interactions, all of which reduce the mobility of epoxy chains around the MWCNT–Mt. However, at high MWCNTs contents, the formation of MWCNTs agglomerates on the surface of Mt sheets may incur the movement of epoxy chains, leading to the reduction in elastic properties.

In addition, the cross-link density (ν_e; mol/L) is also a useful way to evaluate the effect of MWCNT–Mt hybrids on the elastic properties. Based on the rubber elasticity theory, the experimental ν_e can be determined from the rubbery modulus using the following equation [39,40]:

$$\nu_e = \frac{E'_r}{3RT}$$

where E'_r is the storage modulus obtained at $T_g + 40\ ^{\circ}C$ (Pa), R is the gas constant (8.314 L kPa K^{-1}·mol^{-1}), and T is the absolute temperature at $T_g + 40\ ^{\circ}C$ (K). The calculated results of ν_e are displayed in Table 1. By the incorporation of MWCNT–Mt hybrids, the ν_e values of epoxy composites increase considerably. It indicates that MWCNT–Mt hybrids have a pronounced effect on the mechanical properties of resultant composites. The reduction in ν_e for E/M-Mt(0.2:1) may be

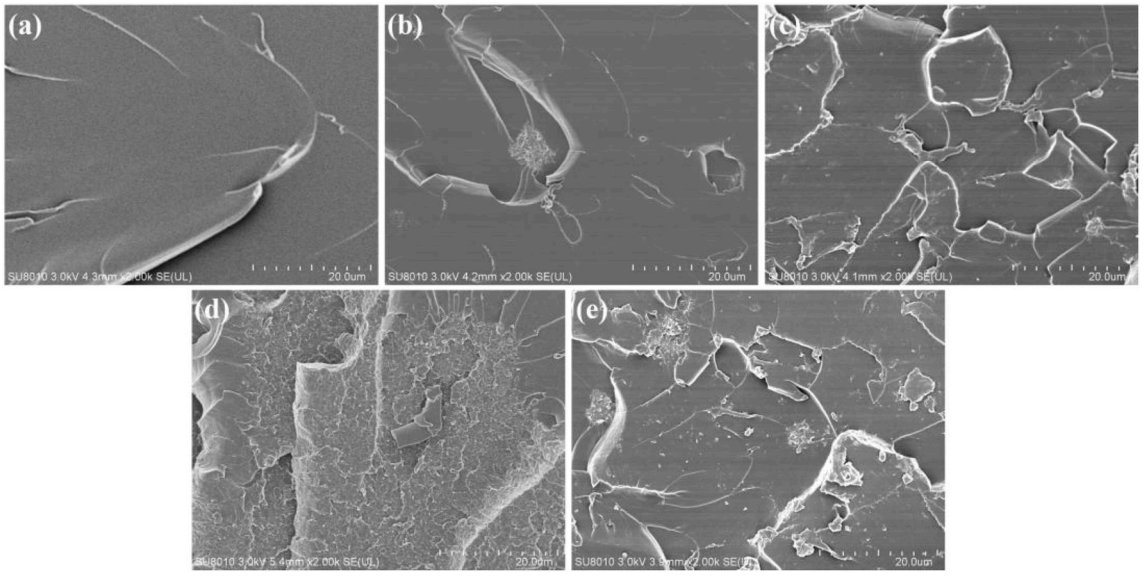

Fig. 7. SEM images of cross-sectional fracture surfaces of tensile samples: (a) Pure EP, (b) E/Mt, (c) E/M-Mt(0.05:1), (d) E/M-Mt(0.1:1) and (e) E/M-Mt(0.2:1).

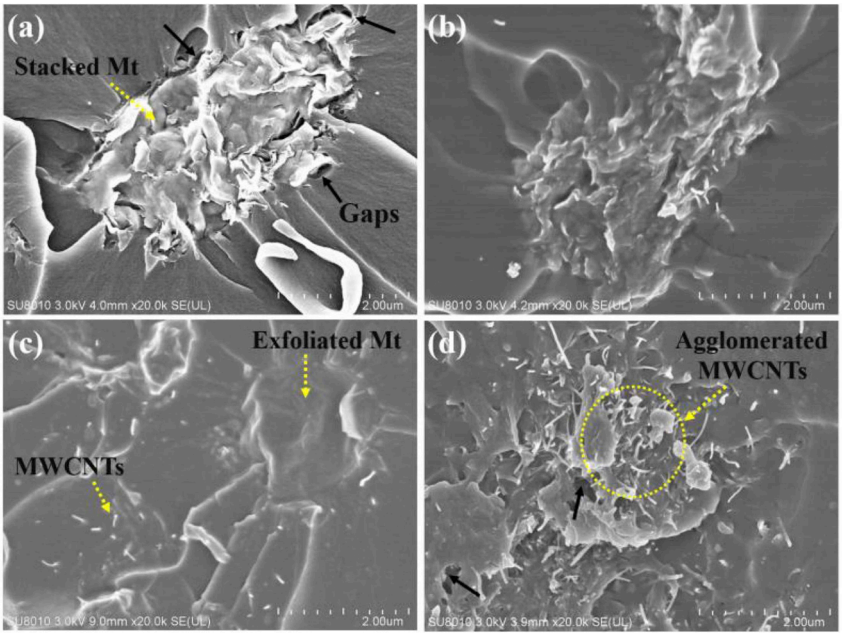

Fig. 8. SEM images showing the interfacial adhesion between MWCNT – Mt and matrix: (a) E/Mt, (b) E/M-Mt(0.05:1), (c) E/M-Mt(0.1:1) and (d) E/M-Mt(0.2:1).

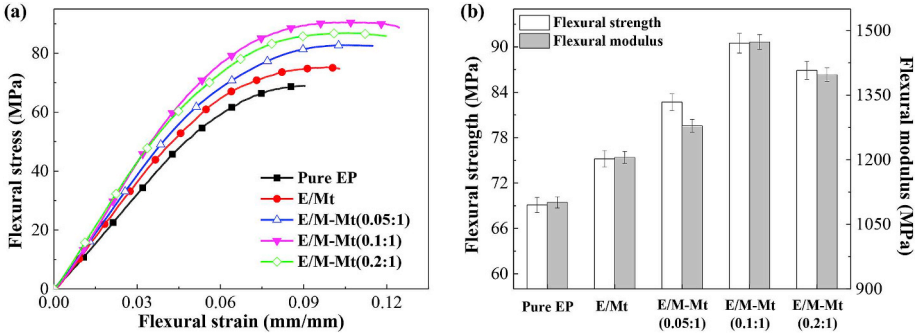

Fig. 9. (a) Stress–strain curves, (b) flexural strength and modulus of epoxy composites containing MWCNT – Mt hybrids with different mass ratios.

attributed to the presence of MWCNTs agglomerates, which leads to the decrease of cross-linking sites in matrix.

It is evident from Fig. 10(b) that the reduction of Tan δ_{max} as well as the positive shift of T_g occurs in epoxy composites. The maximum decrease in Tan δ_{max} is observed for E/M-Mt(0.1:1). Compared with the E/Mt, the Tan δ_{max} of E/M-Mt(0.1:1) is reduced by 29.3%. This behavior can be due to the reduction of mechanical loss in epoxy composites. Also, the maximum increment of T_g (about 7.0 °C) is obtained for E/M-Mt(0.1:1) when compared with the E/Mt. Additionally, the T_r of MWCNT–Mt-filled epoxy composites is 3.3–10.3 °C higher than that of E/Mt, signifying the improvement of thermal stability for epoxy composites. The increase in T_g and T_r can be again explained as the reduction in the mobility of epoxy chains around the MWCNT–Mt hybrids. This phenomenon is attributed to the facts that: (1) the MWCNTs are uniformly dispersed in the matrix; (2) high aspect ratios and large specific surface area of MWCNTs provide the mechanical interlocking with epoxy chains; (3) the covalent bonds between MWCNTs and matrix are created during the curing of resins; (4) an effective barrier effect is given by exfoliated Mt sheets to increase the thermal stability of composites.

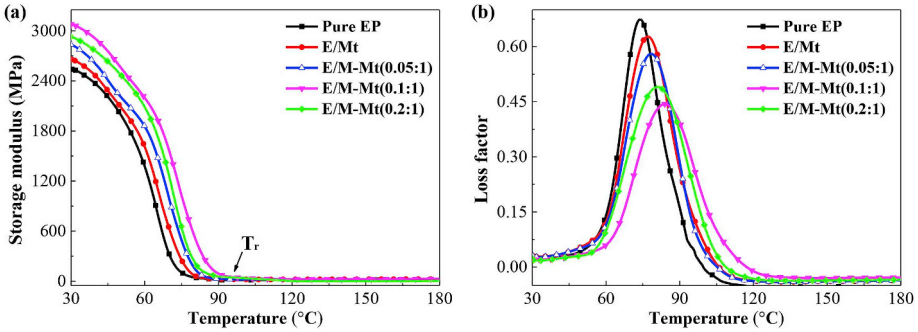

Fig. 10. (a) Storage modulus and (b) loss factor vs. temperature curves of epoxy composites containing MWCNT – Mt hybrids with different mass ratios.

Table 1
DMTA results of epoxy composites containing MWCNT − Mt hybrids with various mass ratios.[a]

Sample	E' at 30 °C (MPa)	ν_e (mol/L)	Tan δ_{max}	T_g (°C)	T_r (°C)
Pure EP	2540	1.549	0.6742	73.82	83.63
E/Mt	2658	2.169	0.6275	76.99	87.92
E/M-Mt(0.05:1)	2841	2.223	0.5804	78.28	91.24
E/M-Mt(0.1:1)	3078	2.432	0.4437	83.97	98.21
E/M-Mt(0.2:1)	2936	2.267	0.4905	81.12	94.56

[a] E', ν_e, Tan δ_{max}, T_g and T_r represent the storage modulus, cross-link density, peak of loss factor, glass transition temperature, and the temperature at which the E' begins to stabilize in the rubbery region, respectively.

4. Conclusions

In this study, the self-assembled MWCNT − Mt hybrids with various mass ratios were designed as reinforcing nanofillers to optimize the structure and mechanical properties of epoxy composites. Based on this design, the dispersion level of MWCNTs and exfoliation degree of Mt in matrix could be also regulated. It was found that the introduction of TETA salts-grafted MWCNTs was beneficial for the dispersion and exfoliation of Mt in matrix; meanwhile, the barrier effect of Mt sheets could assist in the dispersion of MWCNTs in the composites. However, either low or high contents of TETA salts-grafted MWCNTs caused the formation of undesired Mt stacking or MWCNTs agglomerates, respectively. Moreover, the addition of a small amount of MWCNTs reduced the thermal stability of MWCNT − Mt hybrids. With the increase of MWCNTs, the synergistic effect on the dispersibility and thermal stability of MWCNT − Mt hybrids was yielded. Making use of optimal mass ratio of MWCNT:Mt (0.1:1), the MWCNT − Mt hybrid exhibited the lowest mass loss rate and highest decomposition temperatures. Compared with the composite containing pristine Mt, the toughness of epoxy composites containing MWCNT–Mt(0.1:1) exhibited a significant enhancement; the tensile strength, Youngs' modulus and elongation at break were improved by 26.8%, 18.8% and 19.7%, respectively; the flexural strength and modulus were enhanced by 20.4% and 22.3%, respectively; storage modulus in the glassy region was raised by 15.8%.

Acknowledgments

The authors are very grateful for the support by the Fundamental Research Funds for the Central Universities (Grant No. 2018B40814); Postgraduate Research & Practice Innovation Program of Jiangsu Province (Grant No. KYLX16_0734).

Appendix A. Supplementary data

Supplementary data to this article can be found online at https://doi.org/10.1016/j.compositesb.2018.12.028.

References

[1] Ren X, Peng SM, Zhang W, Yi CW, Fang Y, Hui D. Preparation of adipic acid-polyoxypropylene diamine copolymer and its application for toughening epoxy resins. Compos B Eng 2017;119:32–40.
[2] Kim JH, Kwon DJ, Shin PS, Beak YM, Park HS, DeVries KL, et al. Interfacial properties and permeability of three patterned glass fiber/epoxy composites by VARTM. Compos B Eng 2018;148:61–7.
[3] Senthil Kumar MS, Mohana Sundara Raju N, Sampath PS, Chithirai Pon Selvan M. Influence of nanoclay on mechanical and thermal properties of glass fiber reinforced polymer nanocomposites. Polym Compos 2018;39(6):1861–8.
[4] Tsai YT, Chiou JY, Liao CY, Chen PY, Tung SH, Lin JJ. Organically modified clays as rheology modifiers and dispersing agents for epoxy packing of white LED. Compos Sci Technol 2016;132:9–15.
[5] Spinelli G, Lamberti P, Tucci V, Vertuccio L, Guadagno L. Experimental and theoretical study on piezoresistive properties of a structural resin reinforced with carbon nanotubes for strain sensing and damage monitoring. Compos B Eng 2018;145:90–9.
[6] Song PA, Liu LN, Fu SY, Yu YM, Jin CD, Wu Q, et al. Striking multiple synergies created by combining reduced graphene oxides and carbon nanotubes for polymer nanocomposites. Nanotechnology 2013;24(12):125704.
[7] Zeng SH, Shen MX, Duan PP, Lu FL, Chen SN, Xue YJ. Effect of ultrasonic-assisted impregnation parameters on the preparation and interfacial properties of MWCNT/glass-fiber reinforced composites. e-Polymers 2018;18(1):35–47.
[8] Cha J, Jun GH, Park JK, Kim JC, Ryu HJ, Hong SH. Improvement of modulus, strength and fracture toughness of CNT/Epoxy nanocomposites through the functionalization of carbon nanotubes. Compos B Eng 2017;129:169–79.
[9] Kara M, Kırıcı M, Tatar AC, Avcı A. Impact behavior of carbon fiber/epoxy composite tubes reinforced with multi-walled carbon nanotubes at cryogenic environment. Compos B Eng 2018;145:145–54.
[10] Sánchez-Cabezudo M, Prolongo MG, Salom C, Cid MAGD, Masegosa RM. Ternary nanocomposites: curing, morphology, and mechanical properties of epoxy/thermoplastic/organoclay systems. Polym Compos 2015;37(7):95–105.
[11] Zeng SH, Shen MX, Duan PP, Xue YJ, Wang ZY. Effect of silane hydrolysis on the interfacial adhesion of carbon nanotubes/glass fiber fabric-reinforced multiscale composites. Text Res J 2018;88(4):379–91.
[12] Xu LH, Fang ZP, Song PA, Peng M. Functionalization of carbon nanotubes by corona-discharge induced graft polymerization for the reinforcement of epoxy nanocomposites. Plasma Process Polym 2010;7(9–10):785–93.
[13] Guan QB, Yuan L, Zhang Y, Gu AJ, Liang GZ. Improving the mechanical, thermal, dielectric and flame retardancy properties of cyanate ester with the encapsulated epoxy resin-penetrated aligned carbon nanotube bundle. Compos B Eng 2017;123:81–91.
[14] Boccalero G, Jean-Mistral C, Castellano M, Boragno C. Soft, hyper-elastic and highly-stable silicone-organo-clay dielectric elastomer for energy harvesting and actuation applications. Compos B Eng 2018;146:13–9.
[15] Zeng SH, Shen MX, Duan PP, Yang L, Lu FL, Hao LY. Tunable mechanical properties of MWCNT–glass fiber fabric reinforced epoxy composites by controlling MWCNTs dispersing conditions. Compos Interfac 2018;25(10):901–18.
[16] Tüzemen MÇ, Salamcı E, Avcı A. Enhancing mechanical properties of bolted carbon/epoxy nanocomposites with carbon nanotube, nanoclay, and hybrid loading. Compos B Eng 2017;128:146–54.
[17] Al-Saleh MH. Clay/carbon nanotube hybrid mixture to reduce the electrical percolation threshold of polymer nanocomposites. Compos Sci Technol 2017;149:34–40.
[18] Pötschke P, Krause B, Buschhorn ST, Köpke U, Müller MT, Villmow T, et al. Improvement of carbon nanotube dispersion in thermoplastic composites using a three roll mill at elevated temperatures. Compos Sci Technol 2013;74(4):78–84.
[19] Lee SK, Bai BC, Ji SI, In SJ, Lee YS. Flame retardant epoxy complex produced by addition of montmorillonite and carbon nanotube. J Ind Eng Chem 2010;16(6):891–5.
[20] Da-Costa EFR, Skordos AA, Partridge IK, Rezai A. RTM processing and electrical performance of carbon nanotube modified epoxy/fibre composites. Compos Appl Sci Manuf 2012;43(4):593–602.
[21] Madaleno L, Pyrz R, Crosky A, Jensen LR, Rauhe JCM, Dolomanova V, et al. Processing and characterization of polyurethane nanocomposite foam reinforced with montmorillonite–carbon nanotube hybrids. Compos Appl Sci Manuf 2013;44(1):1–7.
[22] Esmizadeh E, Yousefi AA, Naderi G, Milone C. Drastic increase in catalyst productivity of nanoclay-supported CVD-grown carbon nanotubes by organo-modification. Appl Clay Sci 2015;118:248–57.
[23] Manikandan D, Mangalaraja RV, Avila RE, Siddheswaran R, Anathakumar S. Montmorillonite–carbon nanotube nanofillers by acetylene decomposition using catalytic CVD. Appl Clay Sci 2013;71(1):37–41.
[24] Pradhan B, Roy S, Srivastava SK, Saxena A. Synergistic effect of carbon nanotubes and clay platelets in reinforcing properties of silicone rubber nanocomposites. J Appl Polym Sci 2015;132(15):871–82.
[25] Roy S, Srivastava SK, Pionteck J, Mittal V. Montmorillonite–multiwalled carbon nanotube nanoarchitecture reinforced thermoplastic polyurethane. Polym Compos 2016;37(6):1775–85.
[26] Zhao S, Li CY, Zhou Y, Wang SG, Su F, Cui J, et al. A multifunctional hydrogel based on heterostructured hybrids of single-walled carbon nanotubes and clay nanoplatelets. Carbon 2014;77(8):846–56.
[27] Maiti S, Pramanik A, Chattopadhyay S, De G, Mahanty S. Electrochemical energy storage in montmorillonite K10 clay based composite as supercapacitor using ionic liquid electrolyte. J Colloid Interface Sci 2016;464:73–82.
[28] Zeng SH, Shen MX, Yang L, Xue YJ, Lu FL, Chen SN. Self-assembled montmorillonite–carbon nanotube for epoxy composites with superior mechanical and thermal properties. Compos Sci Technol 2018;162:131–9.
[29] Han YQ, Li TX, Gao B, Gao L, Tian XJ, Zhang Q, et al. Synergistic effects of zinc oxide in montmorillonite flame-retardant polystyrene nanocomposites. J Appl Polym Sci 2016;133(10):43047.
[30] Yang L, Qiu JH, Ji HL, Zhu KJ, Wang J. Enhanced dielectric and ferroelectric properties induced by TiO_2@MWCNTs nanoparticles in flexible poly(vinylidene fluoride) composites. Compos Appl Sci Manuf 2014;65:125–34.
[31] Madaleno L, Pyrz R, Jensen LR, Pinto JJC, Lopes AB, Dolomanova V, et al. Synthesis of clay–carbon nanotube hybrids: growth of carbon nanotubes in different types of iron modified montmorillonite. Compos Sci Technol 2012;72(3):377–81.
[32] Wan YJ, Tang LC, Gong LX, Yan D, Li YB, Wu LB, et al. Grafting of epoxy chains onto graphene oxide for epoxy composites with improved mechanical and thermal properties. Carbon 2014;69(2):467–80.
[33] Qian MB, Sun YQ, Xu XD, Liu LN, Song PA, Yu YM, et al. 2D-alumina platelets enhance mechanical and abrasion properties of PA612 via interfacial hydrogen-bond interactions. Chem Eng J 2017;308:760–71.
[34] Kumar A, Ghosh PK, Yadav KL, Kumar K. Thermo-mechanical and anti-corrosive

properties of MWCNT/epoxy nanocomposite fabricated by innovative dispersion technique. Compos B Eng 2017;113:291–9.
[35] Song PA, Xu ZG, Wu YP, Cheng QF, Guo Q, Wang H. Super-tough artificial nacre based on graphene oxide via synergistic interface interactions of π-π stacking and hydrogen bonding. Carbon 2017;111:807–12.
[36] Chen Z, Dai XJ, Magniez K, Lamb PR, Fox BL, Wang X. Improving the mechanical properties of multiwalled carbon nanotube/epoxy nanocomposites using polymerization in a stirring plasma system. Compos Appl Sci Manuf 2014;56(56):172–80.
[37] Tsafack T, Alred JM, Wise KE, Jensen B, Siochi E, Yakobson BI. Exploring the interface between single-walled carbon nanotubes and epoxy resin. Carbon 2016;105:600–6.
[38] Liu WS, Wang YR, Wang PF, Li Y, Jiang QR, Hu XY, et al. A biomimetic approach to improve the dispersibility, interfacial interactions and toughening effects of carbon nanofibers in epoxy composites. Compos B Eng 2017;113:197–205.
[39] Darroman E, Bonnot L, Auvergne R, Boutevin B, Caillol S. New aromatic amine based on cardanol giving new biobased epoxy networks with cardanol. Eur J Lipid Sci Technol 2015;117(2):178–89.
[40] Ding R, Xia Y, Mauldin TC, Kessler MR. Biorenewable ROMP-based thermosetting copolymers from functionalized castor oil derivative with various cross-linking agents. Polymer 2014;55(22):5718–26.